

# Investigation of periodically poled lithium niobate crystals by light diffraction

M. Müller, E. Soergel, and K. Buse<sup>a)</sup>

*University of Bonn, Institute of Physics, Wegelerstrasse 8, 53115 Bonn, Germany*

C. Langrock and M. M. Fejer

*Edward L. Ginzton Laboratory, Stanford University, Stanford, California 94305-4085*

(Received 18 May 2004; accepted 21 November 2004; published online 20 January 2005)

Periodically poled lithium niobate crystals are investigated by illumination along the crystallographic  $c$  axis while applying an external electric field. The resulting diffraction patterns are in good agreement with the results of numerical simulations and directly yield first information such as periodicity, duty cycle, and homogeneity of the domain patterns. © 2005 American Institute of Physics. [DOI: 10.1063/1.1849818]

## I. INTRODUCTION

Recently, periodically poled lithium niobate crystals (PPLN) and periodically poled lithium tantalate crystals (PPLT) have attracted great scientific and commercial interest as important materials in nonlinear optics.<sup>1-3</sup> Consequently, a variety of poling techniques has been developed.<sup>4</sup> To ensure the quality of the generated patterns it is generally necessary to visualize the resulting domain structures. This is normally done by selective etching of the crystals in hydrofluoric acid, which combines a high resolution with a comparative simplicity of use. It is, however, a destructive technique. Although several other nondestructive techniques for the visualization of the domain patterns have been realized such as optical near-field microscopy,<sup>5</sup> scanning force microscopy,<sup>6</sup> or scanning electron microscopy;<sup>7</sup> they all suffer from a long-winded implementation. Furthermore only small sections of the PPLN structures can be investigated by these methods. There is, therefore, still a need for an easy method to visualize large domain patterns.

As an alternative to the established techniques for visualization we have recently proposed a simple method to obtain integrated information about arbitrary domain patterns.<sup>8</sup> In short, illumination of a partially poled lithium niobate or lithium tantalate crystal along the  $c$  axis while simultaneously applying an external electric field generates a star-shaped light-diffraction pattern in the far field of the transmitted beam. This pattern can be attributed to the light diffraction at the domain walls.<sup>9</sup> If an electric field is applied, the electro-optical effect creates a refractive index step at the domain boundaries. Diffraction inside the crystal at this refractive index step distorts the phase of an incoming plane wave. Instead of showing a simple steplike profile, approximately linear changes of the phase over a few micrometers are present. This is analogous to the diffraction at an intensity step (e.g., an opaque half plane), which generates a smooth intensity transition between light and shadow areas. Since light propagates perpendicularly to its phase front, a portion of the light is deflected. Due to the diffraction from

the domain boundaries, the deflected light appears as a ray with a substructure. The deflection always occurs perpendicularly to the domain wall in the direction of the higher index of refraction. The intensity of each individual “ray” is proportional to the total length of domain-walls in the corresponding direction. Therefore, the starlike pattern directly yields the relative distribution of domain-wall orientations in the crystal.

In this paper we report on applying this technique specifically to periodically poled structures. This implementation allows us to extract quantitative information about the domain structures.

## II. METHODS

The experiments are performed with congruently melting, undoped, 0.5-mm-thick,  $z$ -cut, optical grade lithium niobate crystals (supplier: Crystal Technology Inc.). The sign of the spontaneous polarization is periodically inverted using electric-field poling.<sup>10</sup> The crystals are illuminated with the unexpanded beam of an Ar<sup>+</sup> laser (wavelength  $\lambda$ , beam diameter  $\approx 2$  mm) along the optical axis. The  $+c$ -face and the  $-c$ -face of the crystal are contacted by liquid electrodes that allow application of homogeneous electric fields. The far-field light-deflection pattern is observed on a fluorescent screen that is positioned behind the crystal holder (see Ref. 8 for a detailed description of the setup). The electric fields applied are well below the coercive field for both poling directions. Thus, the fields used for this characterization do not change the domain structure. After completing the experiments the crystals are etched in hydrofluoric acid to accurately determine period length and duty cycle of the PPLN crystal.

## III. EXPERIMENTAL RESULTS

Typical far-field light-diffraction patterns behind a PPLN crystal are shown in Fig. 1. The patterns consist of equally spaced diffraction maxima. The angle between the dots is 0.65 at  $\lambda=333$  nm. The size and the relative intensity distribution of each maximum is equal to the size and relative intensity distribution of the incident laser beam. An increase

<sup>a)</sup>Electronic mail: kbuse@uni-bonn.de

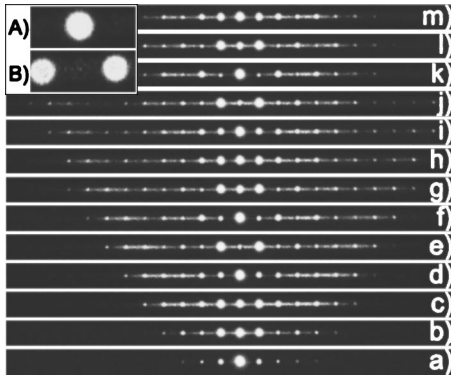


FIG. 1. Typical far-field light-diffraction patterns generated by a PPLN crystal for different applied electric fields. The respective applied voltages go from (a) 0.0 kV to (m) 6.0 kV in 0.5-kV steps. The inset shows the high contrast between the transmitted beam and the +1st and -1st maxima, obtained for voltages of (A) 1.65 kV and (B) 2.45 kV. PPLN period length  $\Gamma=29.5 \mu\text{m}$ , duty cycle  $\kappa \approx 0.5$ , and light wavelength  $\lambda=333 \text{ nm}$ .

of the applied voltage has two effects: the intensity of each maximum changes periodically (the inset in Fig. 1 gives a good example) and higher-order maxima become more pronounced. Both effects become more obvious if the total intensity diffracted into each maximum is plotted versus the applied voltage, as seen in Fig. 2. The intensity of the transmitted beam clearly shows a periodicity as a function of the applied voltage with a period of  $\Delta U \approx 1.2 \text{ kV}$  at  $\lambda=333 \text{ nm}$ . Higher-order maxima show a less regular periodicity, but for increasing voltages  $\Delta U$  is converging towards the value for the 0th order maximum. For the sample shown (with a duty cycle  $\kappa \approx 0.5$ ) the intensity distribution is nearly symmetrical for positive and negative applied voltages.

This behavior can be contrasted with that shown in Fig. 3, which plots the intensity of the transmitted beam versus the applied voltage for three PPLN samples with the same period length but different duty cycles. The more the duty cycle differs from the symmetrical value of  $\kappa=0.5$ , the less symmetrical with regard to the sign of the applied voltage the curves become. In order to get a quantitative measure of this asymmetry we take the difference between the height of the first intensity minimum for negative voltages  $I_0^-$  and the first intensity minimum for positive voltages  $I_0^+$ . This difference is plotted versus the duty cycle in Fig. 4.

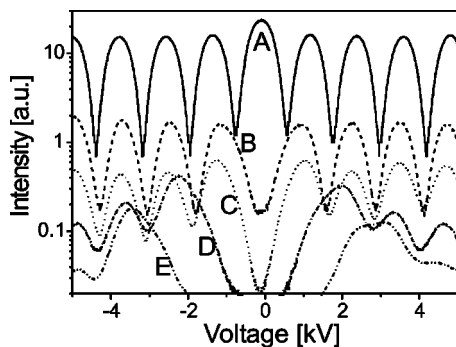


FIG. 2. Diffracted intensity versus the applied voltage for the 0th maximum, i.e., the transmitted beam, curve (A), the 2nd (B), the 4th (C), the 6th (D), and the 8th diffraction maximum (E). PPLN period length  $\Gamma=29.5 \mu\text{m}$ , duty cycle  $\kappa \approx 0.5$ , and light wavelength  $\lambda=333 \text{ nm}$ .

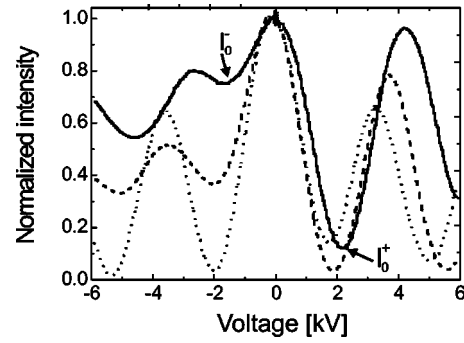


FIG. 3. Transmitted intensity (0th maximum) versus the applied voltage for different duty cycles of the PPLN. The curves correspond to duty cycles  $\kappa$  of 0.2 (solid line), 0.3 (dashed line), and 0.55 (dotted line). For  $\kappa=0.2$  the positions of the first intensity minimum at negative and at positive voltage,  $I_0^-$  and  $I_0^+$ , are marked. PPLN period length  $\Gamma=25 \mu\text{m}$  and light wavelength  $\lambda=455 \text{ nm}$ .

Scattered light is noticeable as a background intensity between the maxima. This background is visible for all investigated samples, although the relative intensity varies from sample to sample and even on different parts of the same sample.

#### IV. DISCUSSION

The reason why periodically poled lithium niobate generates a diffraction pattern of discrete, equally spaced diffraction maxima is simple: An applied electric field causes an electro-optical refractive index grating in the crystal due to the periodic inversion of the electro-optical tensor. Higher-order diffraction occurs because the refractive index grating is nonsinusoidal. The measured diffraction angle  $\beta_n$  of the  $n$ th diffraction maximum for a PPLN crystal with a period length  $\Gamma$  agrees with the theoretical value  $\sin(\beta_n/2) = n\lambda/(2\Gamma)$  from standard diffraction theory. It is also consistent with experimental results reported by Bermúdez *et al.*,<sup>11</sup> who observed the diffraction pattern without an applied voltage. The reason why the diffraction pattern is visible, even without an external voltage, is most likely due to the so-called internal electric fields, which are present in ferroelectric crystals after poling.<sup>12</sup> Those fields are also responsible for shifting the intensity-versus-voltage curves in Figs. 2 and 3 slightly to negative voltages.

To understand the intensity distribution we expand the model that has been presented in Ref. 9 for the light diffraction from a single domain wall. Figure 5(a) shows the light beam directly after passing the PPLN crystal. We still as-

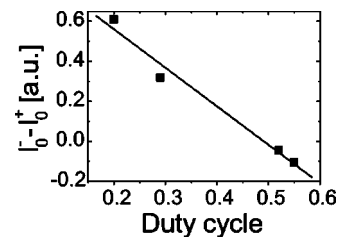


FIG. 4. Intensity difference  $I_0^- - I_0^+$  between the first intensity minima in the transmitted beam at positive and negative values of the applied voltage (see Fig. 3) versus the duty cycle of the PPLN. The solid curve is a linear fit of the data. PPLN period length  $\Gamma=25 \mu\text{m}$  and light wavelength  $\lambda=455 \text{ nm}$ .

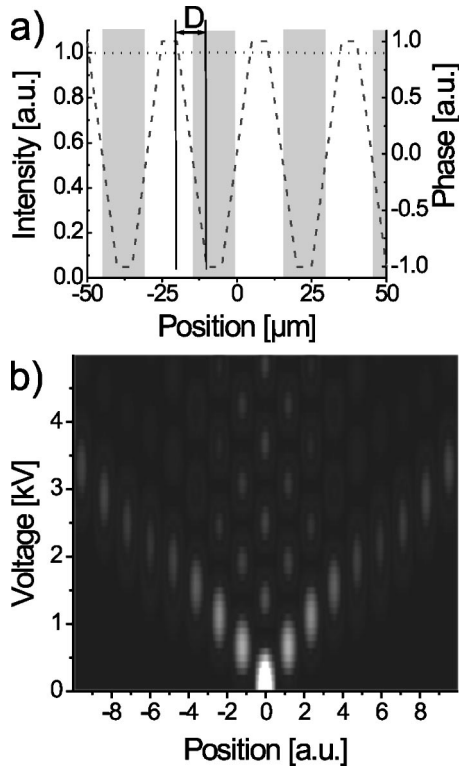


FIG. 5. (a) Spatial distribution of the intensity (dotted curve) and the phase (dashed curve) behind the crystal, which is used to simulate the diffraction pattern. The shaded areas denote the inverted domains. Diffraction inside the crystal is taken into account by assuming an approximately linear phase change over a width  $D$  at the domain wall. (b) Resulting calculated light-diffraction pattern for voltages from 0 to 5 kV.

sume a Gaussian intensity distribution of the beam in the near field. However, the light experiences different optical path lengths in the material depending on the domain orientation due to the different electro-optical refractive index changes, which generates a modulated phase pattern. The phase change is assumed to be continuous at a domain wall over a width  $D$  to account for diffraction inside the crystal. We assume  $D \approx 14 \mu\text{m}$ .<sup>9</sup> Since the electro-optical refractive index change is known, we can use the Rayleigh–Sommerfeld formula to calculate the resulting diffraction pattern [Fig. 5(b)]. This simulated pattern exhibits the same features as the measured one (see Fig. 1). There is a periodic modulation of the intensity of each maximum, where the periodicity  $\Delta U$  is the voltage  $U_{2\pi}$  required for an electro-optical phase shift of  $2\pi$ . Indeed, interferometric measurements of  $U_{2\pi}$  agree with the measured periodicity  $\Delta U$  for all wavelengths investigated. In addition, the simulated pattern shows the observed shift of intensity towards the higher-order maxima. Note that for  $D=0$  (i.e., if we neglect diffraction inside the crystal) this effect disappears and the simulated diffraction intensity pattern repeats itself for increasing voltages of  $I(U) = I(U + U_{2\pi})$ .

According to diffraction theory, the whole intensity should be diffracted into the maxima. However, Fig. 1 shows a distinct intensity background between the maxima. We attribute this background scattering to the fact that our “real” samples are not “ideal” PPLN, as the width of the poled stripes varies slightly. Since we have no samples with clearly

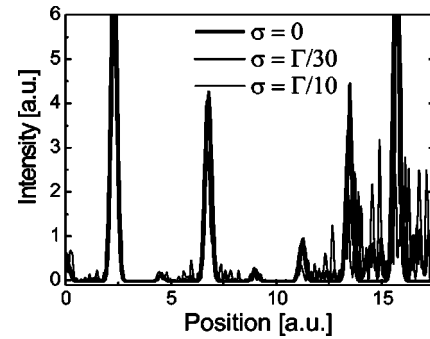


FIG. 6. Simulated intensity distribution of a far-field light-diffraction pattern for an ideal (i.e., perfectly periodic) PPLN crystal and two “real” PPLN crystals, with a statistically fluctuating duty cycle from period to period (with the standard deviation  $\sigma$  given).

defined variations in the periodicity, we check the connection between poling homogeneity and background scattering theoretically. We use the same basic model as in Fig. 5, but now we allow for statistically distributed fluctuations of the duty cycle from period to period. It is unlikely that there are strong fluctuations in the period length since it is given by the periodicity of the lithographic mask. A typical result is given in Fig. 6. It shows part of the simulated intensity diffraction distribution for an ideal periodic crystal and for two crystals with fluctuating duty cycles. The amount of fluctuation is given by the standard deviation  $\sigma$  of the width of the poled stripes (quoted as a fraction of the period length  $\Gamma$ ). The curves show a clear correlation between the crystal inhomogeneity and the background intensity. In fact, we believe that measuring the scattered intensity between maxima is an easy and convenient way to check the PPLN quality.

The basic model, however, cannot explain the differences in the diffraction pattern between positive and negative applied voltages that appear for PPLN crystals with a duty cycle of  $\kappa \neq 0.5$ , as seen in the Figs. 3 and 4. That is because the model simply superposes the influence of separate domain walls on the incident wave. It does not take into account the diffraction on more than one domain boundary and clearly breaks down if the domain width becomes approximately equal to or smaller than the diffraction width  $D$ . To simulate the diffraction pattern in this case it is necessary to accurately simulate the light diffraction inside the crystal, which is beyond the scope of this paper. It is, however, intuitively clear that different diffraction patterns for positive and negative voltages can occur. The small domains can work as waveguiding structures if the index of refraction is higher inside those structures. This has, e.g., been shown for small-sized domains in lithium tantalate crystals.<sup>13</sup> For duty cycles of  $\kappa \neq 0.5$  the waveguiding properties of the PPLN structure therefore depend on the sign of the applied voltage. This changes the light patterns directly behind the crystal and finally the light-diffraction patterns. However, even without a comprehensive model, measuring the intensity versus the applied voltage for the transmitted beam could be a simple and reliable way to determine the duty cycle of a PPLN crystal as soon as calibration curves (such as Fig. 4) for the relevant period length become available.

In addition the setup used might be of interest as an

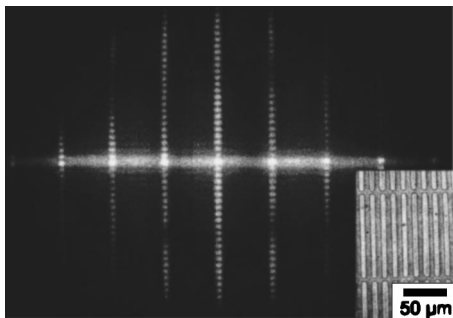


FIG. 7. Typical far-field light-diffraction pattern generated by a two-dimensional PPLN crystal. The inset shows a part of the domain pattern of the crystal that has been made visible by chemical etching. Applied voltage  $U=6$  kV, light wavelength  $\lambda=455$  nm, and PPLN period lengths  $\Gamma_1=12$   $\mu\text{m}$  and  $\Gamma_2=100$   $\mu\text{m}$ .

electro-optical beam modulator, since the degree of modulation of the transmitted beam is nearly 100% and the transmitted intensity is completely independent of the light polarization. Its major disadvantage would be the high modulation voltage. However, since the voltage needed is independent of the beam size it might be a viable scheme for the modulation of large beams. If losses of 50% are acceptable it might even be used for beam switching.

## V. GENERALIZATION TO TWO-DIMENSIONAL PPLN

So far, we have investigated standard one-dimensional periodically poled lithium niobate crystals. The same method can be used for more complex periodic domain patterns. Figure 7 shows an example of a two-dimensional PPLN crystal and a respective light-diffraction pattern. The two period lengths of  $\Gamma_1=12$   $\mu\text{m}$  and  $\Gamma_2=100$   $\mu\text{m}$  are clearly represented in the diffraction pattern. Also, all other features and explanations should be directly transferable to the two-dimensional case.

## VI. CONCLUSION

Passing coherent light along the  $c$ -axis through a periodically poled lithium niobate or lithium tantalate crystal while simultaneously applying a homogeneous electric field well below the coercive field yields diffraction patterns that allow *in situ* determination of period length, duty cycle, and homogeneity of the domain pattern. A numerical or—even better—analytical description of the light diffraction from domain boundaries in PPLN crystals can help to explore further the applicability of the method presented in this paper for a study of the quality of PPLN domain structures, but in any case the experimental accuracy will determine to which extend conclusions can be drawn. Thus the limits given by an experimental calibration of the method cannot be overcome by a theoretical analysis.

## ACKNOWLEDGMENTS

Financial support by the DFG and the Deutsche Telekom AG is gratefully acknowledged. This research was supported in part by the US Army Research Office through ARO Grant No. DAAD19-03-1-0199.

- <sup>1</sup>M. M. Fejer, G. A. Mangel, D. H. Jundt, and R. L. Byer, *IEEE J. Quantum Electron.* **28**, 2631 (1992).
- <sup>2</sup>L. E. Myers, R. C. Eckardt, M. M. Fejer, R. L. Byer, W. R. Bosenberg, and J. W. Pierce, *J. Opt. Soc. Am. B* **12**, 2102 (1995).
- <sup>3</sup>K. R. Parameswaran, M. Fujimura, M. H. Chou, and M. M. Fejer, *IEEE Photonics Technol. Lett.* **12**, 656 (2000).
- <sup>4</sup>M. Hou and P. D. Townsend, *J. Phys. D* **28**, 1747 (1995).
- <sup>5</sup>T. J. Yang, V. Gopalan, P. J. Swart, and U. Mohideen, *Phys. Rev. Lett.* **82**, 4106 (1999).
- <sup>6</sup>R. Lüthi, H. Haefke, K.-P. Meyer, L. Howald, and H.-J. Güntherodt, *J. Appl. Phys.* **74**, 7461 (1993).
- <sup>7</sup>B. J. Wicks and M. H. Lewis, *Phys. Status Solidi A* **26**, 571 (1986).
- <sup>8</sup>M. Müller, E. Soergel, and K. Buse, *Opt. Lett.* **28**, 2515 (2003).
- <sup>9</sup>M. Müller, E. Soergel, M. C. Wengler, and K. Buse, *Appl. Phys. B: Lasers Opt.* **78**, 367 (2004).
- <sup>10</sup>G. D. Miller, R. G. Batchko, W. M. Tulloch, D. R. Wiese, M. M. Fejer, and R. L. Byer, *Opt. Lett.* **22**, 1834 (1997).
- <sup>11</sup>V. Bermúdez, A. Gil, L. Arizmendi, J. Colchero, A. M. Baró, and E. Diéguez, *J. Mater. Res.* **15**, 2814 (2000).
- <sup>12</sup>V. Gopalan and M. C. Gupta, *J. Appl. Phys.* **80**, 6099 (1996).
- <sup>13</sup>M. Müller, E. Soergel, and K. Buse, *Appl. Opt.* **43**, 6344 (2004).